Werk

Jahr: 1985
Kollektion: fid.geo
Signatur: 8 Z NAT 2148:56
Digitalisiert: Niedersächsische Staats- und Universitätsbibliothek Göttingen
Werk Id: PPN1015067948_0056
PURL: http://resolver.sub.uni-goettingen.de/purl?PPN1015067948_0056

LOG Id: LOG_0032
LOG Titel: Large-scale studies of Pi-2's associated with auroral breakups
LOG Typ: article

Übergeordnetes Werk

Werk Id: PPN1015067948
PURL: http://resolver.sub.uni-goettingen.de/purl?PPN1015067948
OPAC: http://opac.sub.uni-goettingen.de/DB=1/PPN?PPN=1015067948

Contact

Niedersächsische Staats- und Universitätsbibliothek Göttingen
Georg-August-Universität Göttingen
Platz der Göttinger Sieben 1
37073 Göttingen
Germany
Email: gdz@sub.uni-goettingen.de

J Geophys (1985) 56: 133–145

Journal of Geophysics

Large-scale studies of Pi-2's associated with auroral breakups

J.C. Samson
Institute of Earth and Planetary Physics, Department of Physics, University of Alberta, Edmonton, Alberta, Canada T6G 2J1

Abstract. In the interval 22–27 October 1979, an observational campaign was conducted to study the correlation of substorm-triggered geomagnetic pulsations (Pi 2's) and auroral breakups. This campaign took advantage of the North American magnetometer networks which were operated during the International Magnetospheric Study. Data from 28 magnetometer stations ranging from 73.9°–38.9° N (centred dipole) were used in this study, 20 of which yielded high time resolution data which permitted proper analysis of Pi 2's.

An analysis of two substorm onsets indicates that the Pi 2''s occurred in conjunction with the brightening of a quiet arc, near the equatorward border of visible auroral activity. One breakup occurred within the region of the ambient, eastward ionospheric electrojet, suggesting that the onset of the Pi 2's and the substorm current systems can occur equatorward of the Harang discontinity. Plots of the intensities and polarizations of the Pi 2's indicate that a substantial part of the Pi 2's magnetic field comes from field-aligned and ionospheric currents associated with the substorm onset.

A comparison of the polarizations of the Pi 2's with those computed from a simple model of ionospheric and field-aligned currents indicates that the Pi 2's in this study might be caused by the motion of a transient current system with a westward velocity of 20–50 km/s.

Key words: Aurora – Substorm – Pi 2 pulsation – Polarization – Electrojets

Introduction

Pi 2 geomagnetic pulsations are directly connected with auroral brightening and the onset of polar magnetic substorms (Troitskaya and Gul'elmi, 1967; Afanasyeva et al., 1970; Pytte and Trefall, 1972; Pytte et al., 1976). At the onset of the substorm, expansive phase enhanced field-aligned currents (FAC) flow into and out of the auroral ionosphere. Although changes in this FAC propagate, in part, as shear Alfvén waves (e.g. Mallinckrodt and Carlson, 1978), much of the upward current over an auroral arc is carried by electrons with energies of several keV (Vondrak, 1975) and, consequently, some of the magnetic transients associated with Pi 2's might be produced by precipitating high-energy electrons.

In this study, I would like to show that the morphology of Pi 2 magnetic fields is dominated by FACs and ionospheric currents near brightening arcs. In an attempt to explain the data I shall also propose a simple model for the Pi 2 currents near the brightening arc. This heuristic model gives a reasonable prediction of the Pi 2 polarizations and fields, suggesting that the Pi 2's might be associated, in part, with the currents (and possibly high-energy electrons) which cause the arc brightening.

There is already considerable evidence that even mid- and low-latitude Pi 2's are a direct result of high-latitude FACs, with two dominant FAC regions, associated in part with the substorm current wedge (Björnsson et al., 1971; Samson and Harrold, 1983; Lester et al., 1983). The above studies are either statistical in nature or limited to one geomagnetic region (e.g. midlatitudes). The study presented here gives relatively complete coverage of high- and mid-latitude Pi 2's for individual substorm expansive phase onsets and arc brightenings.

The experiment

The auroral campaign was conducted in the interval 22–27 October 1979. The campaign was designed to take advantage of the data from the IMS magnetometer array and from the University of Alberta magnetometer array before it ceased operation in late autumn, 1979. These data were complemented by magnetometer data from the Air Force Geophysics Laboratory (AFGL) stations in the United States. Because of data transmission and noise problems, only nine IMS stations yielded data which were suitable for the analysis of substorm electrojets and Pi 2 polarizations. Data from seven standard Canadian observatories were also used to determine the configuration of the substorm electrojets, but not the polarizations of the Pi 2's.

The centred dipole coordinates (Hakura, 1965) of all the stations and observatories used in this study are given in Table 1. Figure 1 presents a map of the centred dipole coordinates of the 20 stations used to determine the spectral characteristics and polarizations of the Pi 2's.

Table 1. Coordinates of stations and observatories

Code	Station	Centred dipole coordinates	
		North	East
University of Alberta stations			
PROV	Fort Providence	67.5	292.2
SMIT	Fort Smith	67.3	300.1
LEDU	Leduc	60.6	303.0
FTCH	Fort Chipewyan	66.1	301.0
Standard Canadian Observatories			
	Victoria	54.3	294.2
	Meanook	61.9	301.1
	Yellowknife	69.1	294.6
	Cambridge Bay	76.8	296.8
	Great Whale River	66.6.	348.8
	Ottawa	56.7	352.8
	Baker Lake	59.9	325.3
	Fort Churchill	68.7	322.8
AFGL stations			
NEW	Newport	55.2	299.3
RPC	Rapid City	53.3	319.0
CDS	Camp Douglas	54.5	334.5
MCL	Mt. Clemens	53.6	343.9
SUB	Sudbury	53.6	358.4
LOC	Lompoc	41.4	302.1
TPA	Tampa	38.9	345.8
IMS stations			
CPY	Cape Perry	73.9	274.1
AVI	Arctic Village	68.1	284.7
COL	College	64.8	282.9
TLK	Talkeetna	63.0	283.1
GIM	Gilliam	66.3	325.3
NOW	Norman Wells	69.2	279.6
FSP	Fort Simpson	67.2	287.7
TUC	Tucson	40.5	313.3
BOU	Boulder	48.7	317.9

Throughout the discussion, coordinates are centred dipole coordinates, and time is universal time (UT), unless otherwise indicated.

A manually operated, wide-angle camera was located at Fort Smith for the auroral photography. This camera had a field of view of 105° and exposure time of 5-20 s. In addition, an observer's log was kept of the observations at this site.

Reduction of data

All the magnetometer data from the Alberta, IMS and AFGL array were recorded in digital form and then sampled at a 10 s interval (each channel) for this study, even though the recorded data often had a smaller sample interval. This sample interval (10 s) gives a Nyquist frequency of 50 mHz which is well above Pi 2 frequencies (5-15 mHz). All the data presented in this study have been rotated to correspond to centred dipole coordinates, with H magnetic north (centred dipole), D magnetic east, and Z downward.

Five representations of the magnetic field data were used in this study. These representations include:

a) standard magnetograms
b) high-pass-filtered-(5 mHz) magnetograms
c) latitude profiles
d) difference-equivalent currents and
e) spectral representations with estimates of power spectra and polarization parameters.

The standard magnetograms show the recorded magnetic fields in H, D, Z (centred dipole) coordinates, with *no absolute baseline.* The high-pass-filtered data are useful for locating Pi 2's in the data (low-frequency substorm fields are removed), and these data are also used as input to the program which determines the spectral representation.

Both the latitude profiles and the equivalent currents used difference values of the magnetic field in order to estimate the configurations of the substorm currents. The latitude profiles were computed only near the Alberta array, and used the stations NEW, LEDU, FTCH, SMIT as well as the standard observatories at Meanook, Yellowknife and Cambridge Bay. For these profiles, a quiet-time baseline (H, D and Z) was subtracted from the fields recorded during a substorm or substorms. The difference values were then plotted as a function of latitude. These profiles are often easy to interpret as the ionospheric currents typically flow east-west. However, near the front of the westward-travelling surge (WTS), the profiles can be difficult to interpret. Note also that since these profiles used a quiet-time baseline, the inferred currents contain other existing current systems in addition to the desired substorm currents.

Conversely, the equivalent current representations used in this study attempted to isolate the currents for single substorms. Difference values of the magnetic fields in H and D were computed by subtracting base values from 2 min before the substorm onset (as determined by the Pi 2 onset) from field values during the substorm. The vector perturbations were then rotated 90° clockwise (viewed downward) in order to estimate equivalent "sheet" currents flowing in the ionosphere.

The polarization characteristics of the Pi 2's were computed in the spectral (Fourier transform) domain because of the band limited nature of these pulsations (see the examples to be given below). Also, since the magnetic data are typically noisy, the polarization parameters were calculated using statistical methods to determine estimators. Complete details are given in Samson and Harrold (1983) or Samson (1983a). The parameters presented in this study are:

a) The power spectra $\mathbf{z}^{\dagger}(j)\mathbf{z}(j)$, where

$$\mathbf{z}(j)=\sum_{t=0}^{N-1}\mathbf{x}(t)\exp(-2\pi ijtN^{-1})$$

and

$$\mathbf{x}^{\mathrm{T}}(t)=[H(t), D(t), Z(t)].$$

The power spectra are the sums of the frequency dependent power on all three components of the magnetometer.

b) The pure state power spectra, $\hat{a}^2(k)\hat{\mathbf{u}}^{\dagger}(k)\hat{\mathbf{u}}(k)$ (Samson and Harrold, 1983, Eqs. A7 and A8). The

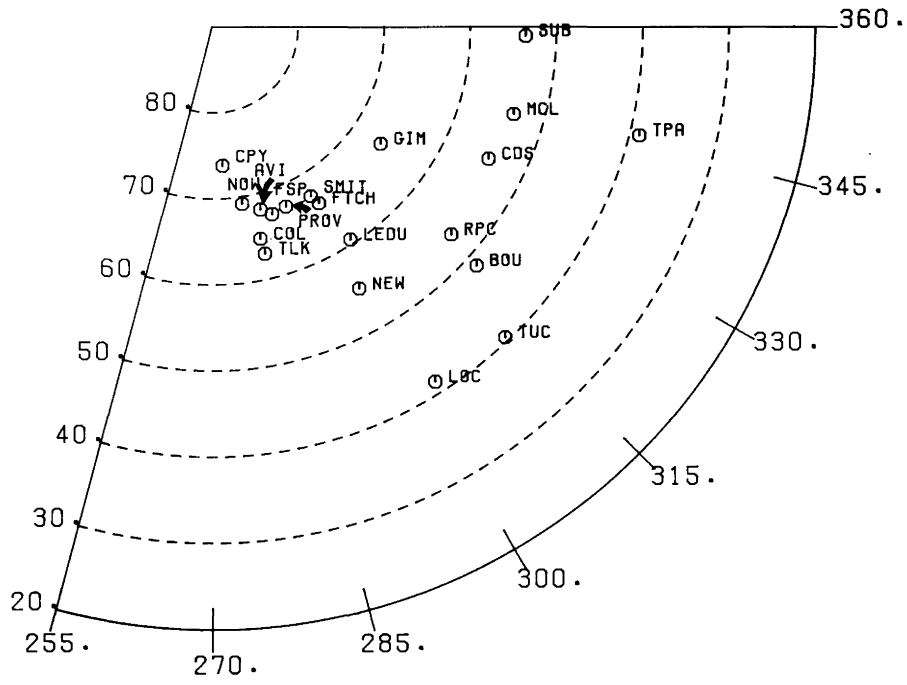

Fig. 1. A map of the positions of the magnetic stations used in this study. Standard observatories are not included. Centred dipole coordinates are used

pure state power spectra estimate the power in the "coherent" waves like Pi 2's, with "noise" power removed.

c) The degree of polarization estimator $\hat{B}_1^2$ (Samson and Harrold, 1983, Eq. A6).

d) The parameters of the polarization ellipse in the horizontal $(H-D)$ plane, including the ellipticity (ratio minor axis to major axis) and orientation of the polarization ellipse (direction of major axis) [Samson and Harrold, Eqs. (1), (2) and (3)]. The polarization ellipses are estimated from the spectra and cross spectra (of the pure states).

Note that the power spectra a) are unsmoothed. The estimators of the pure states were calculated using a spectral window with seven degrees of freedom (complex Wishart sense). If the signal is a pure state or totally polarized, then $\hat{B}_1^2 = 1$. Conversely, if data comprise isotropic noise, then $\xi\{\hat{B}_1^2\} \simeq 0.06$ (Samson, 1983b), where ξ denotes expectation.

In processing the auroral photographs, both slides and enlarged prints were made. The borders of the aurorae were digitized by tracing over the photographs on a flat bed digitizer. These data were then mapped to centred dipole coordinates by assuming the height of the auroral luminosity to be 100 km.

Observations

Auroral activity

The nights of October 22, 23 and October 23, 24 had considerable cloud cover at Fort Smith (SMIT) and consequently no magnetic data from these nights were analysed. The night of October 24, 25 did, however, yield an excellent series of photographs of auroral breakups. The descriptions which follow are based on the observer's log and the photographs from SMIT.

The first visible aurora occurred at ~2:30 UT October 25 (20:24 local time, October 24), with a long arc north of zenith (at SMIT), running east-west. The growth of this arc was followed by patchy brightening to the east. At 2:38 a faint arc formed near the southern horizon. By 3:12 the northern arc had moved overhead. Between 3:12 and ~6:32 the arc remained approximately overhead with variable intensity and some brightening and structure.

At ~6:32 a diffuse arc began forming near the southern horizon. This arc brightened considerably at 6:33 and then expanded northward, indicating the beginning of an auroral breakup. Unfortunately, this event was out of the field of view of the camera. However, the magnetic data showed a clear substorm onset and consequently Pi 2 data for this event were analysed.

By 6:56 the auroral activity had died down and only a quiet arc could be seen near the southern horizon. At ~7:04 the southern arc began to brighten again, and a second breakup followed. A mapping of the brightened arc is given in Fig. 2. As shown later, this breakup event started near 60°-61° N and by 7:15 the auroral activity had expanded to ~65° N. A note of caution should be included here, however, as there was also considerable auroral activity far to the west after the beginning of the breakup. This breakup seems to be only part of a much larger increase in auroral and magnetic activity.

The rest of the night had variable auroral activity, most consisting of patchy and structured arcs overhead. No distinct breakup events were seen.

Magnetic activity

Selected magnetograms from Newport (NEW) and the Alberta array for the intervals near the two breakups discussed above are given in Fig. 3. Inspection of the trace at LEDU shows clear negative H excursions at both 6:33 and 7:04 (arrows) in conjunction with the auroral breakups. This indicates that the Alberta array

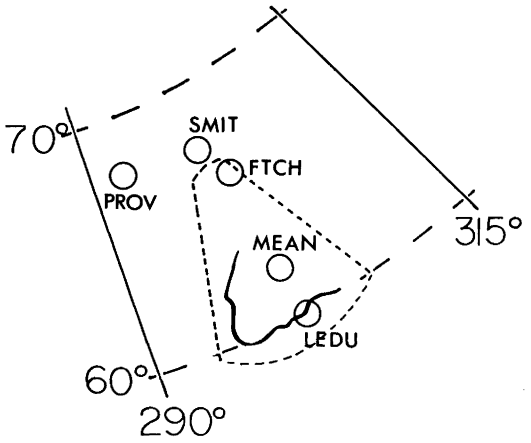

Fig. 2. A map in centred dipole coordinates of the position of the border of the aurora at 7:15 UT. The *dotted line* indicates the field of view of the camera

was situated over the substorm-enhanced westward electrojet, to the east of any WTS. The negative Z component at LEDU and the positive Z component at FTCH indicate that both breakups occurred to the north of LEDU but south of FTCH (see the latitude profiles to be presented later).

Before continuing in a discussion of the two events, some comment should be made about the ionospheric electrojets before the substorm onsets. A latitude profile from the Alberta array and nearby observatories for 6:00 is given in Fig. 4. To the south of approximately 64° N, all the H components are positive, indicating the presence of an *eastward* electrojet flowing south of a large westward electrojet (negative H). Near the boundary between these electrojets there is a level shift of about 90 nT in the D component. This level shift might be caused by upward FAC. This upward FAC and the transition from eastward to westward electrojets are all signatures of the Harang discontinuity (Rostoker et al., 1975). Consequently, the southern arcs mentioned in the auroral observations were south of the Harang discontinuity.

The eastward electrojet remained stable until the breakup event at 6:33 (note the stable H component at LEDU in Fig. 3). Consequently, this auroral breakup appears to have begun just south of the Harang discontinuity, driving a wedge of westward electrojet into the region south of the discontinuity and then moving the discontinuity westward. These observations are consistent with those of Baumjohann et al. (1981).

Figure 5 (top) shows the equivalent currents for the first breakup event. A strong electrojet extended from ~345° to 300° E at ~61°–62° N. These equivalent currents indicate that the event was fairly well localized near the Alberta array.

The equivalent currents for the second event (Fig. 5, bottom) show that the electrojets in this event were far more widespread, with the largest electrojet strengths at the westernmost stations near ~68° N (particularly AVI). The westward electrojet was centred near 61°–62° N at 300° E, shifting northward to ~68° N at ~275° E. This event also had considerably more structure in the directions of the equivalent currents, with some suggestion of a developing eastward electrojet to the south of the strong westward electrojet.

Latitude profiles at 7:03 and 7:14 (Fig. 6) show that a well-defined westward electrojet was associated with the second breakup near the Alberta array. A slight D level shift near the northern border of the westward electrojet at 7:03 indicates that these stations were near a region of *downward* FAC, in contrast to the upward FAC at 6:00 (Fig. 4). These features, and auroral obser-

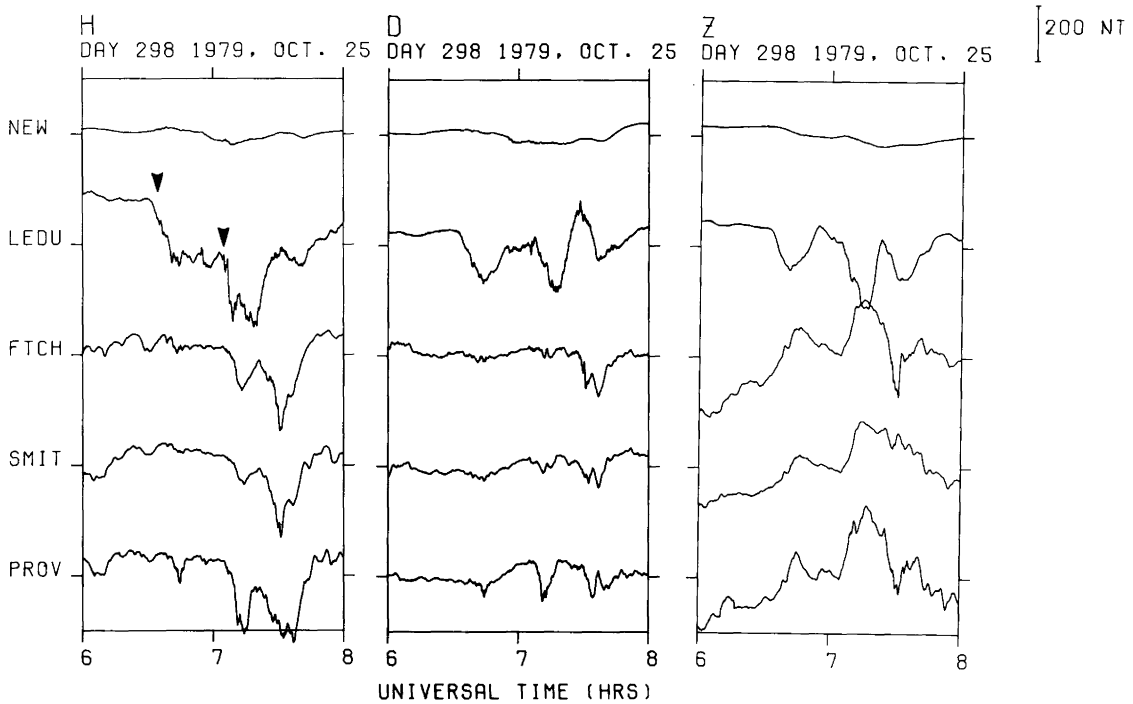

Fig. 3. Magnetograms from the Alberta array and NEW. Centred dipole coordinates are H – magnetic north, D – magnetic east and Z – downward

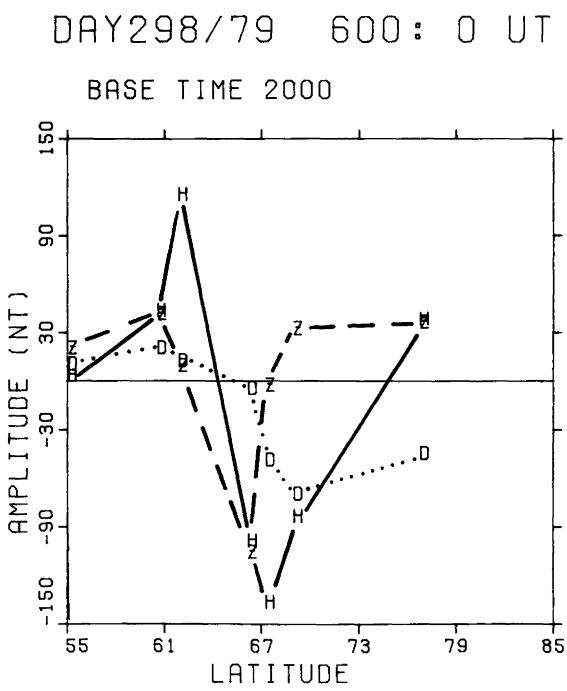

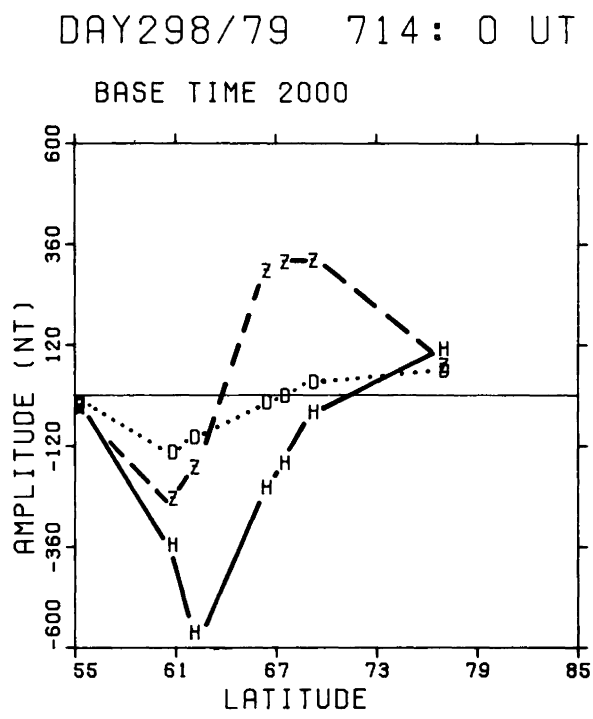

Fig. 4. Latitude profiles at 06:00 October 25. Base time was 20:00 October 24

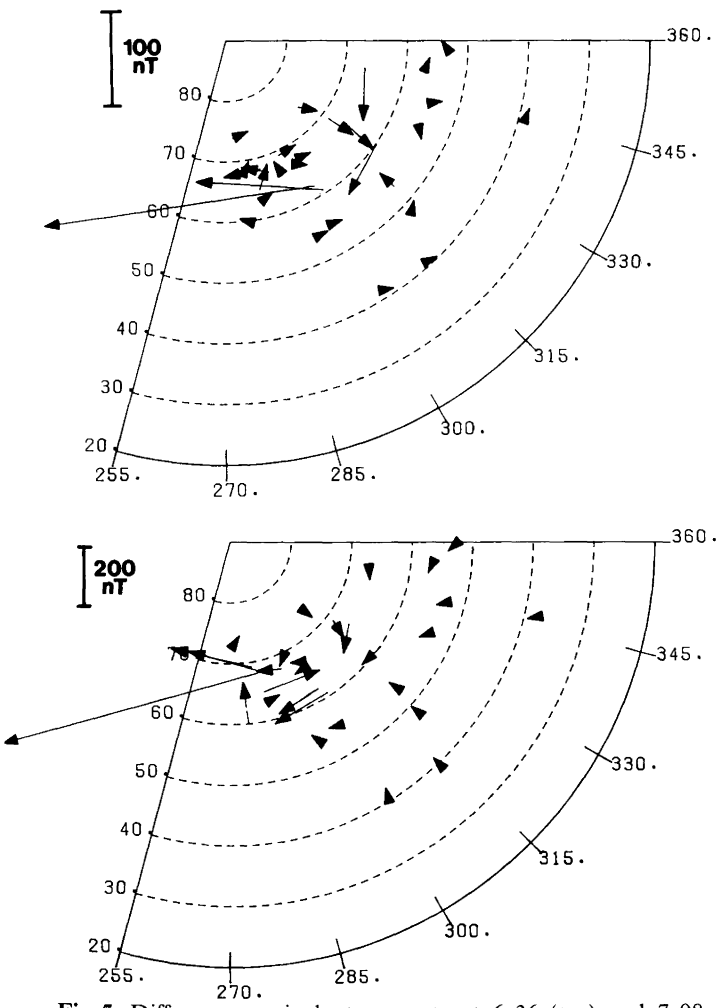

Fig. 5. Difference equivalent currents at 6:36 (*top*) and 7:08 (*bottom*)

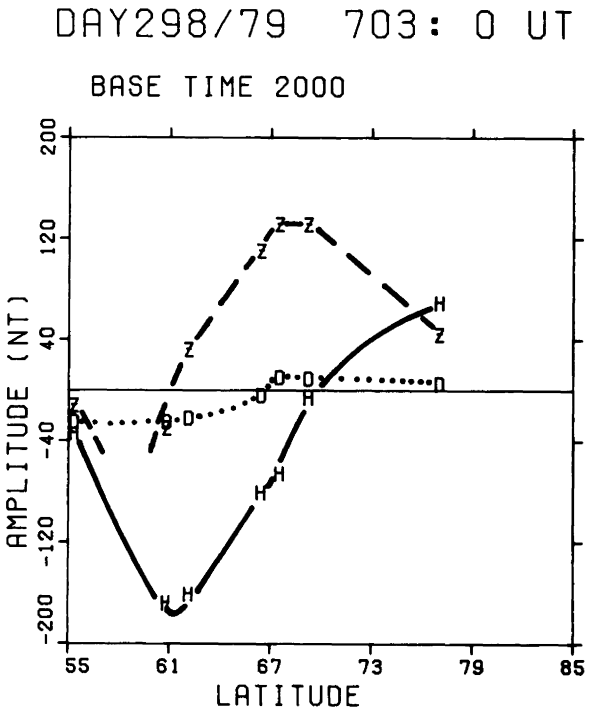

Fig. 6. Latitude profiles at 7:03 and 7:14

vations, suggest that the centre of the breakup activity may have been considerably to the west (see Fig. 2 in Samson and Rostoker, 1983).

Even though the auroral map (Fig. 2) shows a large north-south feature to the west of the Alberta array, these latitude profiles are compatible with an electrojet flowing almost directly westward and centred near 60°–63°. Thus the magnetic fields at the Alberta array appear to be entirely due to currents flowing near the

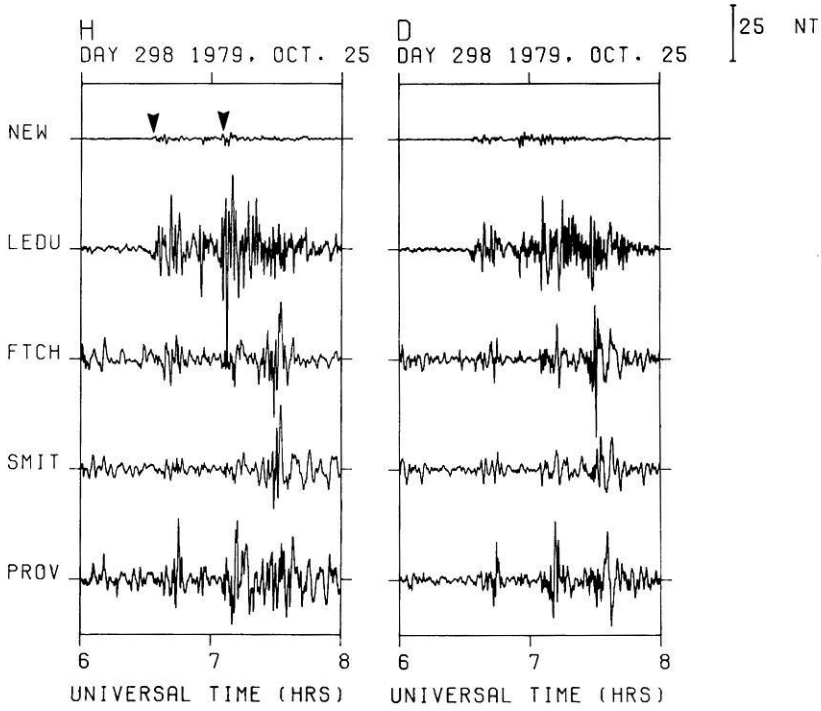

Fig. 7. High pass (5 mHz) filtered data for the H and D components of the Alberta array and NEW. The *arrows* indicate the Pi 2 onsets at NEW

low-latitude (60°–61°) part of the arc, which extended in an east-west direction.

Pi 2 pulsations

High-pass-filtered data for the interval 06:00–08:00 are given in Fig. 7. Clear Pi 2's were associated with both breakups and are easiest to see at NEW (see arrows on the diagram). The extreme complexity of the wave forms at FTCH, SMIT and PROV emphasizes the difficulties in estimating the parameters of Pi 2's recorded by stations near the breakup.

Figure 8 summarizes the characteristics of the Pi 2 associated with the 6:33 breakup (no auroral photos are available). Power spectra over the interval 6:30–6:45 indicate that this Pi 2 pulsation train had a mean frequency of about 10 mHz. A comparison of the contours of the pure state power in Fig. 8 (top) with the equivalent currents in Fig. 5 (top) shows that the region of the substorm westward electrojet, and the peak in the Pi 2 power, overlapped. In this study we do not have sufficient latitudinal resolution to determine whether the Pi 2 peak was actually south of the centre of the electrojet as found by Rostoker and Samson (1981). The data in Fig. 8 also indicate that the centre of the Pi 2 activity did not extend beyond the westernmost stations.

Values of the degree of polarization, $\hat{B}_1^2$ (10 mHz), are contoured in Fig. 8 (middle). Near the western edge of the enhanced westward electrojet, $\hat{B}_1^2$ drops to very low values ($\hat{B}_1^2 \simeq 0.2$) indicating that the Pi 2 here was obscured by noise. This is perhaps not surprising since this might be near the region of the formation of the WTS. The FAC and electrojets associated with the WTS contribute large amounts of noise to the ULF magnetic spectrum (Samson and Rostoker, 1983; Samson and Harrold, 1983).

The highest value of $\hat{B}_1^2$ (~ 0.8) occurred just equatorward of the centre of activity of the Pi 2. This characteristic most likely arises from the fact that stations at these positions see only the integrated effects of FAC associated with the Pi 2, and not the more detailed spatial and temporal structures in the electrojets and high-latitude FAC. Also, the high-latitude regions see more dynamic motions of the Pi 2 sources (Samson and Rostoker, 1983) and this can make the high-latitude Pi 2's look unpolarized.

The polarization ellipses in the $H-D$ plane for the 6:33 event are plotted in Fig. 8 (bottom). There are only two regions with CW (clockwise viewed down) polarization; one centred near the maximum in the Pi 2 activity and the other at the two easternmost stations. Except possibly for the data at the two easternmost stations, these data are consistent with the statistical picture given by Samson and Harrold (1983). The two easternmost stations are much further from the substorm onset than any of the data used by Samson and Harrold. A more detailed evaluation of these polarization data will be given later in the discussion section of the manuscript.

The Pi 2 associated with the 7:04 breakup has been analysed in somewhat more detail because of the availability of the auroral photographs for correlative purposes. Some representative power spectra ($\mathbf{z}^\dagger \mathbf{z}$) for this event are given in Fig. 9 (top). The spectral peak of the Pi 2 (~ 9 mHz, marked by arrow) is quite prominent at the mid-latitude station NEW. At LEDU, the peak is less prominent, but the peak power increased. The station LEDU is near the latitude of the onset. At the highest latitude station PROV, the Pi 2 peak cannot be clearly identified except by correlating it with the peaks at the other two stations.

The pure state powers are shown in Fig. 9 (middle). Now the Pi 2 peaks at NEW and LEDU are even more

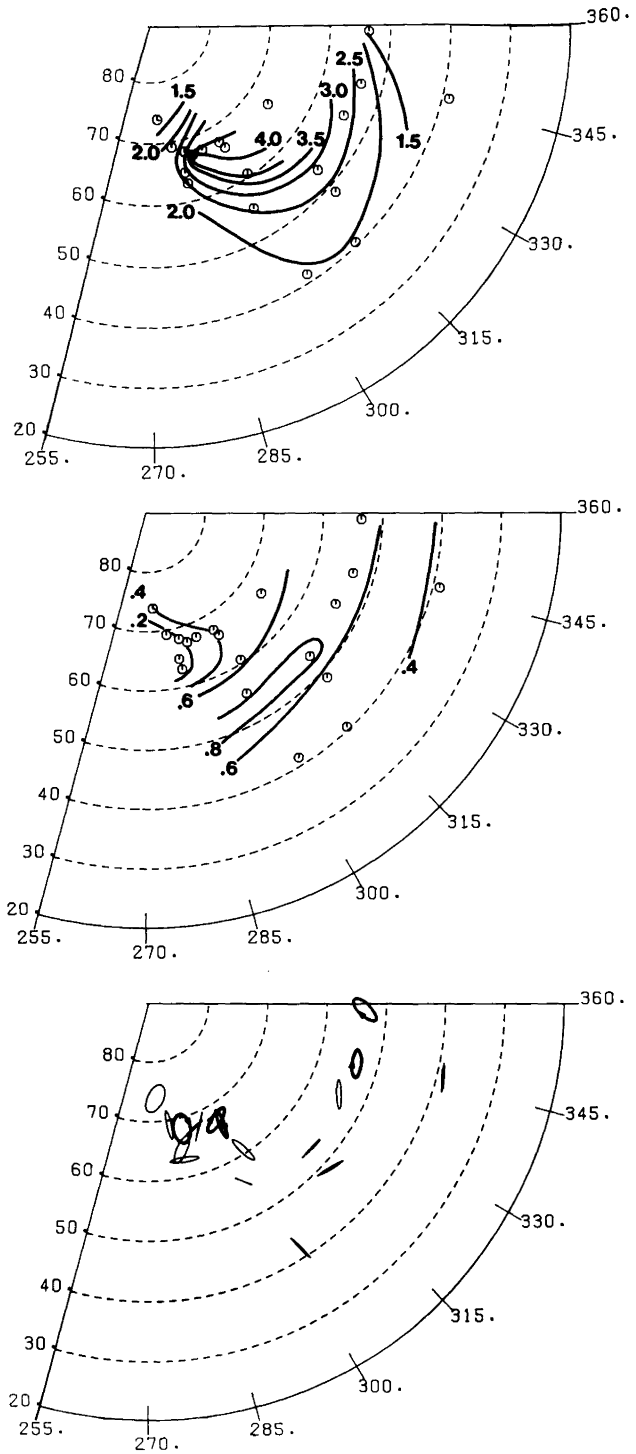

Fig. 8. Power and polarization parameters for the Pi 2 in the interval 6:30–6:45, at 10 mHz. *Top:* log pure state power ($\log_{10} \hat{a}\hat{\mathbf{u}}^{\dagger}\hat{\mathbf{u}}$). *Middle:* degree of polarization estimates, $\hat{B}_1^2$. *Bottom:* the polarization ellipses in the horizontal plane. A dark ellipse with an arrow indicates CW polarization, otherwise the polarization is CC

prominent, since the Pi 2's appear highly polarized. The peak at PROV is more clearly resolved, though it is still difficult to identify. The Pi 2 is somewhat easier to find by inspecting plots of $\hat{B}_1^2$ against frequency. These plots for the three stations are given in Fig. 9 (bottom). At NEW the Pi 2 had a $\hat{B}_1^2$ in excess of 0.8 and the

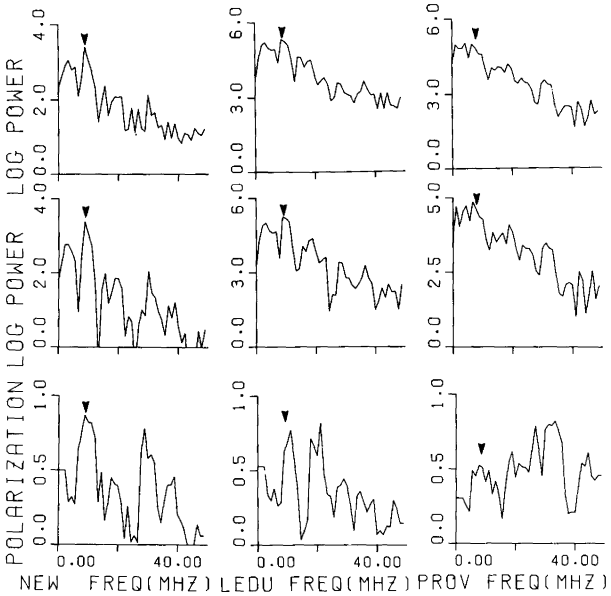

Fig. 9. *Bottom:* polarization spectra $\hat{B}_1^2$ for the second Pi 2 (7:02–7:17). *Middle:* pure state power spectra. *Top:* power spectra ($\mathbf{z}^{\dagger}\mathbf{z}$)

peak is very prominent. At LEDU, the Pi 2 was also highly polarized ($\hat{B}_1^2 \simeq 0.7$) and is clearly visible on the plot. A pulsation with a frequency near 20 mHz shows even higher degrees of polarization. At PROV, the Pi 2 had $\hat{B}_1^2 \simeq 0.5$, but the Pi 2 peak is quite visible. Note once again the very highly polarized waves occupying a band from ~20–30 mHz. These high-frequency pulsations probably are not directly connected to the Pi 2 source mechanism and consequently I shall not consider them here.

The contours of the powers of the Pi 2 associated with the second breakup, given in Fig. 10 (top), show that this Pi 2 had a very large longitudinal extent. Also, the maximum did not occur over the area of magnetometer coverage, but possibly further to the west. The maximum was well localized latitudinally and seems to coincide with the substorm-enhanced electrojet (Fig. 5, bottom) and with the position of the brightened arc in the vicinity of the Alberta array (Fig. 2). These data show that the centre of activity was west of the stations (west of 270° E). This agrees with the interpretation of the latitude profile in Fig. 6 (bottom), where the *D* level shift indicated downward FAC. Thus the auroral features in Fig. 2 are only part of a complex and extended breakup.

The contours of $\hat{B}_1^2$ (Fig. 10, middle) show that this event has many similarities to the previous event. The highest polarizations are found to the south of the intensity maximum. In this case, however, the lowest values are found not near the western edge of the array of stations, but to the southwest of the intensity maximum. This region of low polarity coincides with the northward and eastward equivalent currents shown in Fig. 5 (bottom) and is due west of the extended northward arc in Fig. 2. Consequently, this region of low polarization might have been caused by a localized WTS.

The polarization ellipses for the Pi 2 associated with

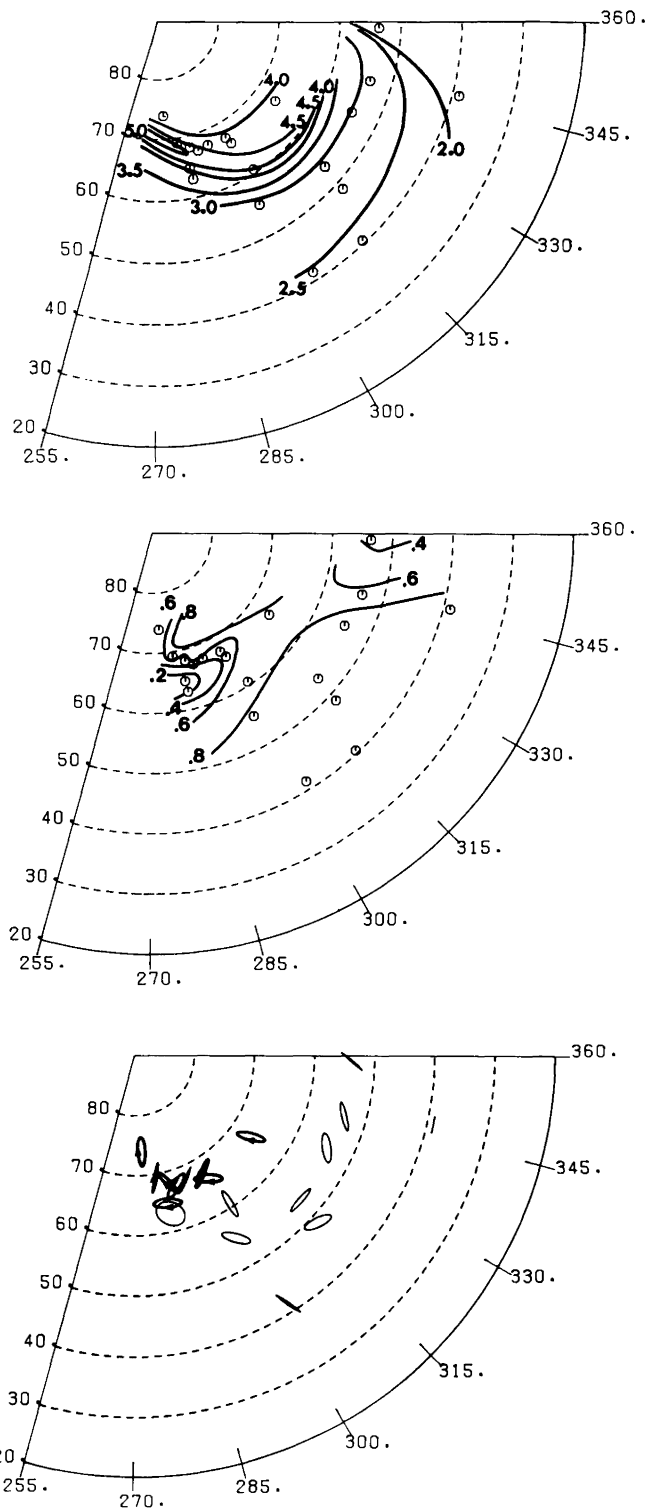

Fig. 10. Power and polarization parameters for the Pi 2 in the interval 7:02–7:17, at 9 mHz. *Top:* log pure state power. *Middle:* $\hat{B}_1^2$. *Bottom:* the polarization ellipses

the second event are plotted in Fig. 10 (bottom). All stations south of ~64° N show CC (counterclockwise) polarization, indicating, as shown later, westward propagation of a region of FAC at high latitude. A more detailed evaluation of the polarization data is given in the discussion to follow.

Discussion

Before continuing the appraisal of the data in this study, it is essential that we consider existing, theoretical constructs for the generation of Pi 2's. A substantial number of theories have been developed, but the complexity of the FAC and ionospheric currents associated with the substorm expansive phase has proven to be a formidable obstacle to the development of complete and self-consistent theories.

It is now generally accepted that the enhanced FAC associated with the expansive phase must propagate, at least initially, as shear Alfvén waves (Maltsev et al., 1974; Mallinckrodt and Carlson, 1978; Southwood and Stuart, 1979). However, nearer the ionosphere, this enhanced FAC can lead to the formation of electrostatic shocks, double layers, anomalous resistivity, of kinetic Alfvén waves (see e.g. Kindel and Kennel, 1971; Kan, 1975; Shawhan et al., 1978; Mozer et al., 1980; Goertz, 1981). Any of these mechanisms can lead to the formation of the beams of electrons (in keV range) which cause the auroral arc brightening associated with the substorm expansive phase. These beams of energetic electrons often carry a large part of the upward FAC associated with an auroral arc (Vondrak, 1975). Consequently these high-energy electrons might contribute to a large part of the Pi 2's magnetic field.

The precipitating electrons in the arc cause increases in the ionospheric conductivities. These increases in the conductivity lead, in turn, to rapid changes in the configuration of ionospheric currents associated with the auroral arc. In addition, changes in the horizontal gradients of the conductivities lead to changes in the FAC associated with the arc. Transient changes in the ionospheric currents and FAC contribute to part of the Pi 2's magnetic field near the brightening arc (Samson and Rostoker, 1983).

It appears unlikely that the mechanism for the formation of Pi 2's can be separated from the mechanism leading to FAC and arc brightening during the substorm expansive phase. Consequently, we are led to consider a complex sequence of interactions, some using kinetic theory, others using magnetohydrodynamic (MHD) theory. It is doubtful that MHD theory alone can give an answer to all the observed features of Pi 2's, at least at high latitudes. Boström (1975) has reviewed the complexity of the interactions in magnetospheric-ionospheric coupling. All of the complexities inherent in ionospheric current and FAC systems associated with the substorm expansive phase probably apply to Pi 2's as well

To discuss the transient FAC and ionospheric currents associated with Pi 2's it is perhaps most informative to begin with the cold plasma equations in the magnetosphere. Then the changing electric field $\mathbf{E}e^{i\omega t}$ is governed by the vector-equation (see Stix, 1962)

$$\nabla\times\nabla\times\mathbf{E}-\frac{\omega^2}{c^2}\mathbf{K}\mathbf{E}=\mathbf{0}, \tag{1}$$

where, in the low frequency limit ($\omega \ll$ ion cyclotron frequency), the equivalent dielectric tensor $\mathbf{K}$ is given by

$$\mathbf{K}\approx\mathrm{diag}\,[c^2/v_a^2, c^2/v_a^2, -\omega_{pe}^2/\omega^2]. \tag{2}$$

In Eq. (2), c is the speed of light, v_a is the Alfvén speed, ω_{pe} is the electron plasma frequency and the geomagnetic field is $\mathbf{B}_0 = [0, 0, B_3]$.

The problem now is to choose suitable boundary conditions and geometries for the sources of the changing electric fields and FAC associated with the substorm expansive phase and Pi 2's. Some evidence now suggests that the source of FAC near the Harang discontinuity, and the region 1 currents of Iijima and Potemra (1976), is a velocity shear zone associated with the low-latitude boundary layer (LLBL) and the outer region of the central plasma sheet (CPS) (Sonnerup, 1980; Rostoker, 1983, 1984; Rostoker and Samson, 1984). The anti-sunward convention in the LLBL leads to electric fields which map to equatorward, ionospheric electric fields, poleward of the Harang discontinuity in the evening sector. The sunward convection in the CPS leads to poleward, ionospheric electric fields in regions equatorward of the Harang discontinuity.

The data from this campaign and the observations of Baumjohann et al. (1981) indicate that at least some of the onsets of substorm expansive phases can occur in association with quiet arcs which are equatorward of the Harang discontinuity. Consequently, the Pi 2's and substorm expansive phases might be connected with changes in the convective velocity of plasma in the CPS, and possibly near the LLBL. Rostoker et al. (1984) have suggested that some of the substorm energy might be derived from a slowing of the sunward convective velocity in the CPS.

A slowing of the sunward convective velocity will be accompanied by a transient electric field, which maps to an *equatorward transient* electric field, superposed on the poleward convection field in regions of the ionosphere, equatorward of the Harang discontinuity. For convenience and simplicity here, I shall initially adopt a Cartesian geometry and return to a dipolar geometry for numerical modelling. In the magnetotail, near the LLBL, vectors in the x_1 direction are perpendicular to $\mathbf{B}_0$, pointing in the direction (dawn to dusk) of the cross-tail electric field. In the ionosphere, I shall assume that x_1 is magnetic north, x_2 is magnetic east, and x_3 is in the direction of $\mathbf{B}_0$. I shall also assume that the arc is aligned east-west and consequently gradients $\frac{\partial}{\partial x_1} \gg \frac{\partial}{\partial x_2}$. This inequality of the gradients is also true for regions near the LLBL, where the convective velocities show considerable shear in the x_1 direction (Eastman et al., 1976). Also, in association with the convective flow $E_1 \gg E_2$, ($\mathbf{E} \simeq -\mathbf{v} \times \mathbf{B}_0$).

Now, neglecting terms that are second order in E_2 and $\partial/\partial x_2$, the third component of Eq. (1) is

$$\frac{\partial^2 E_3}{\partial x_1^2} - \frac{\partial^2 E_1}{\partial x_1 \partial x_3} - \frac{\omega_{pe}^2}{c^2} E_3 = 0. \tag{3}$$

Equation (3) indicates that the parallel electric field E_3 is coupled to E_1 through electron plasma oscillations and the FAC is carried by electrons. Parallel electric fields associated with localized Alfvén waves were noted by Fejer and Lee (1967). Normally $E_3 \ll E_1$. However, if $\partial/\partial x_1$ is large, then the parallel electric fields at the leading edge of a wavefront can accelerate electrons to hundreds of eV (Goertz and Boswell, 1979).

Before the wavefront reaches the ionosphere, any FAC carried by electrons is fed by polarization currents (perpendicular to $\mathbf{B}_0$)

$$j_p = (\mu_0 v_a^2)^{-1} \frac{\partial \mathbf{E}_1}{\partial t}. \tag{4}$$

When the wave reaches the ionosphere, the polarization currents are replaced by Hall and Pedersen currents (see e.g. Nishida, 1978, Chap. III.5) and the impedance mismatch leads to reflected waves propagating up the field lines. In the model I am considering here, the gradients in the Hall and Pedersen conductivities are perpendicular to the quiet arc and consequently $\nabla \sigma_{H,P} \times \mathbf{E}_\perp = \mathbf{0}$, where σ_H and σ_P are the Hall and Pedersen conductivities, respectively. Then

$$E_{1R}(x_1) = \left[\frac{(\mu_0 v_a)^{-1} - \Sigma_P(x_1)}{(\mu_0 v_a)^{-1} + \Sigma_P(x_1)}\right] E_{1I}(x_1), \tag{5}$$

where R and I indicate reflected and incident, respectively, and Σ_P is the height-integrated Pedersen conductivity (Glassmeier, 1984). Since Σ_P is normally much greater than $(\mu_0 v_a)^{-1}$, the reflected wave has E_{1R} positive or poleward. (Note that the incident wave is a transient with equatorward $\mathbf{E}_{1I}$.)

The FAC associated with the waves is given by the relation (see e.g. Kan et al., 1982)

$$\begin{aligned} j_3(x_1) &= (\mu_0 B_0 v_a)^{-1} \left[\hat{\mathbf{n}}_R \cdot \mathbf{B}_0 \frac{\partial E_{1R}(x_1)}{\partial x_1} + \hat{\mathbf{n}}_I \cdot \mathbf{B}_0 \frac{\partial E_{1I}(x_1)}{\partial x_1}\right] \\ &\approx (\mu_0 B_0 v_a)^{-1} \left[\hat{\mathbf{n}}_R \cdot \mathbf{B}_0 \frac{\partial E_{1R}(x_1)}{\partial x_1}\right], \end{aligned} \tag{6}$$

where $\hat{\mathbf{n}}$ is a unit vector in the direction of propagation. In making the approximation in Eq. (6), I have assumed $\frac{\partial E_{1R}}{\partial x_1} \gg \frac{\partial E_{1I}}{\partial x_1}$, due to the large gradients in conductivities near the arc. Since $E_{1R}(x_1)$ is positive everywhere (i.e. points poleward near the ionosphere), $\frac{\partial E_{1R}(x_1)}{\partial x_1}$ is negative on the field lines threading the poleward border of the arc and positive on the equatorward border. Consequently FAC flows downward on field lines threading the poleward side of the arc and the region of enhanced conductivity and upward on equatorward field lines.

To model the Pi 2 magnetic fields, the finite scale sizes in the east-west (x_2) directions must, in reality, be considered. These finite east-west dimensions lead to east-west offsets in the FAC, due to the Hall conductivity in the arc (normally $\Sigma_H > \Sigma_P$). Consequently the downward FAC will tend to be somewhat to the east of the upward FAC (see e.g. Samson, 1982, Fig. 8). Note also that the configuration of FAC that is discussed here is compatible with the features of the substorm current "wedge" (McPherron et al., 1973) and the formation of a transient westward electrojet (see Fig. 11).

In order to compute the magnetic fields and polarizations associated with the transient FAC, the FAC

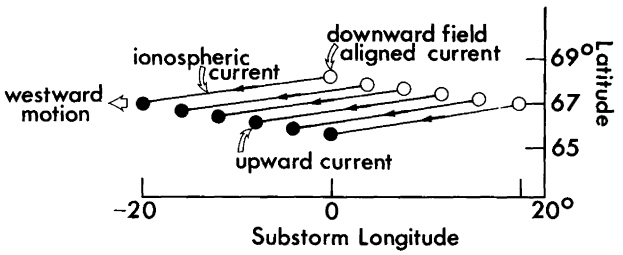

Fig. 11. A model current system for the numerical calculation of Pi 2 magnetic fields. The ionospheric currents flow at a height of 110 km

and ionospheric current model in Fig. 11 have been used. This model is meant to retain the essential features of the reflected electric fields and FAC. The Alfvén velocity near the ionosphere is very high (~1,000–3,000 km/s), and since Pi 2's have time scales on the order of tens of seconds or greater, the high latitude Pi 2 magnetic field can be derived from a model with no phase changes along a current loop.

Ionospheric currents were deduced by assuming a conductivity ratio $\Sigma_H/\Sigma_P=5$ (Brekke et al., 1974), $\nabla\times\mathbf{E}\simeq\mathbf{0}$, with $\mathbf{E}$ (sum of incident and reflected) in the ionosphere pointing equatorward. The FAC sheets at the edge of the region of enhanced conductivity were approximated by the set of six discrete FAC systems (for numerical computations). A dipolar geometry was used for the FAC. The magnetic fields associated with the currents were calculated using programs similar to those discussed by Kisabeth (1979). The FAC were integrated to the magnetic equator (dipole field). Although the model is somewhat nonphysical in the geometry of the ionospheric currents, this feature will not compromise the interpretation as I tend to use this only as an heuristic model to approximate the Pi 2 oscillations.

Many observations indicate that Pi 2 fields show westward apparent phase velocities (Lester et al., 1983 and references therein). Also, since the Pi 2 currents at a given location are transient in nature, the current system in Fig. 11 moves westward to produce the oscillating Pi 2 fields seen on the ground. This westward motion correspond to a *sunward* propagation of the slowing of convection in the CPS. The entire current system moves westward at a constant velocity but with diminishing strength. Note that the current system does not oscillate in the moving frame. Pashin et al. (1982) used a similar principle in modelling Pi 2 magnetic fields. For the simulation, the velocity was chosen to be 4° longitude/time step, and the longitudinal attenuation was exp(-longitude/7)^2. The scale size (−20° to 20° longitude) was based on the observations of Samson and Harrold (1983).

To visualize how this model can produce oscillating fields, it is best to consider a point to the southwest of the start of the current system. An observer at that station will see an "apparent" substorm current wedge moving westward, with oscillations in the H component; negative, positive, negative in that sequence. The D component will be 90° out of phase (D is zero when H is maximum) leading to the elliptical polarizations seen at mid latitudes.

To maintain compatibility with the experimental results for the Pi 2 polarizations in this study and that of Samson and Harrold (1983), I have calculated the polarizations of the model Pi 2 fields by using the same procedure as that used for the observations (see Samson and Harrold, 1983, Appendix). Figure 12 gives the estimated polarizations for the model. Near and to the west of the initial onset the polarization pattern is fairly complex because of the mixture of magnetic fields from FAC and ionospheric currents (see the description in Samson and Rostoker [1983]). Clockwise polarization occurs directly equatorward of the initial upward FAC, and CC directly poleward. This reversal is caused by a latitudinal change in the direction of the magnetic field of the FAC, whereas the fields from the electrojet show little latitudinal phase shift. In most other regions (away from onset), the magnetic fields are dominated by those from the FAC and show CC polarization equatorward of 64° and CW poleward of 68° latitude.

The orientations of the major axis clearly show the substorm "wedge" effect, with the axis oriented to be compatible with two regions of FAC near the onset. This pattern results from the attenuation of the Pi 2 currents with distance westward. Also note that in Fig. 11, the sheets of FAC are slightly tilted from east-west orientation. This tilt was added to give better agreement with the results of Samson and Harrold (1983).

A detailed comparison of the polarization data in Figs. 8 and 10 with the model parameters in Fig. 11 indicates that the model is compatible with many of the polarization features of the Pi 2's in this study. The maximum powers of the Pi 2's occur in and near the brightening arc and the enhanced substorm expansive phase electrojets (at least to the resolution of the station spacing of this study). I could find no secondary maxima in the total pure state power ($H+D+Z$) in regions equatorward of the brightening arc and the primary maximum of the Pi 2 power. In the model, the northern border of the region of CW polarization, which is centred near the breakup, is near the northern border of the enhanced westward electrojet associated with the Pi 2. Accordingly, the two northernmost stations (NOW, CPY) in Fig. 8, which are far north of the substorm-enhanced electrojet (see Fig. 5), had CC polarization while those closer to the electrojet (AVI, FSP, PROV, SMIT, FTCH) had CW polarization. Also, all stations which were well south of the enhanced electrojet have CC polarization as the model predicts (except MCL and SUB). Unfortunately, no data could be obtained for stations in the region 60°–75° N, 315°–345° E, in order to determine whether the region of CW polarization predicted for high latitudes does in fact occur in this event.

The polarizations of the second Pi 2 (Fig. 10) also appear to match those in the model. All stations south of ~64° N show CC polarization, indicating westward propagation of the high-latitude FAC associated with the Pi 2. Near the region of the intensity maximum of the Pi 2's and the region of the substorm westward electrojet, the polarizations are predominatnly CW. In this case, the breakup electrojet and Pi 2 maximum were too far north for the high-latitude region of CC polarization to be seen.

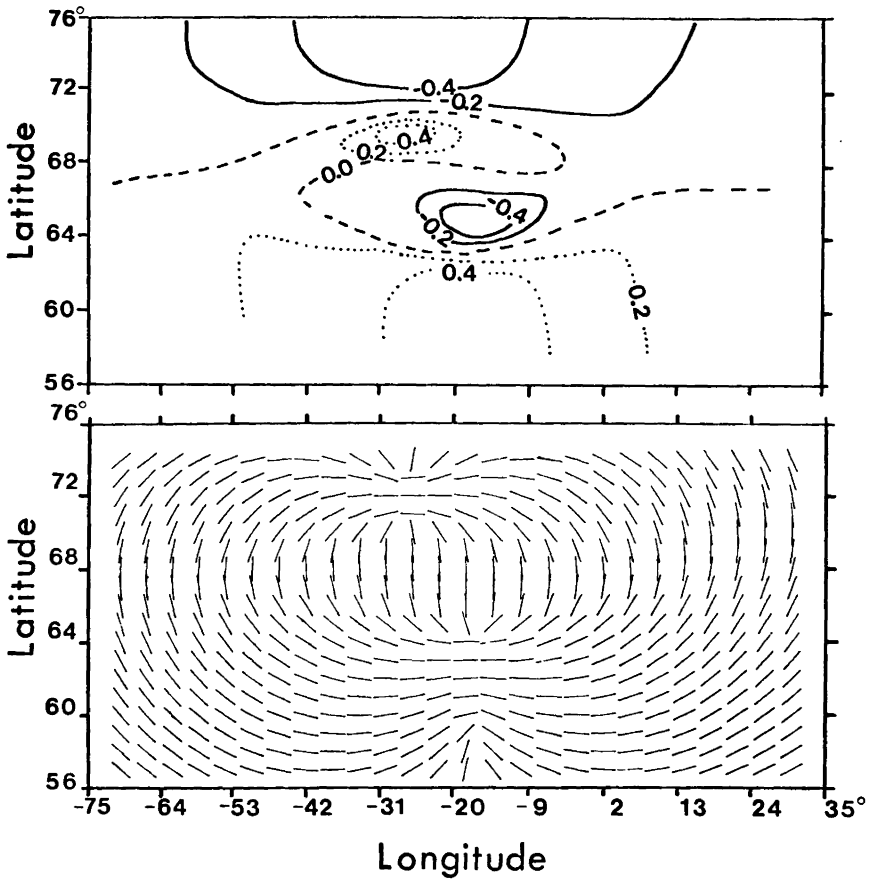

Fig. 12. Polarizations for the Pi 2 model. *Top:* Ellipticity (ratio minor to major axis). Positive and negative ellipticities denote CC and CW polarization, respectively. *Bottom:* Orientations of the major axes of the polarization-ellipses

Turning to the orientations of the polarization ellipses, the major axis in both events appear to be aligned in a manner that suggests a region of FAC somewhere near ~65° N. For the first Pi 2 (Fig. 8) the FAC occurs over the longitudinal range ~300° to 330°, whereas for the second Pi 2 (Fig. 10) the longitudinal range is larger, ~270° to 340°. Inspection of the model polarizations (Fig. 12, bottom) indicates that this must be the region of net *downward* FAC.

The region of CW polarization near the location of the onset of the substorm expansive phase shows that both the ionospheric electrojets and FAC contribute to the polarizations in this region. South of the intensity-maximum, all polarizations are CC and this is consistent with a westward moving FAC system at high latitudes. Unfortunately, this campaign was limited to events which showed only the net downward FAC, because the cameras were placed near the western part of the array.

To produce the observed mid-latitude frequencies (9–10 mHz) of the Pi 2's, the westward velocity of the FAC associated with the Pi 2 must be near 20–50 km/s. I have computed this velocity by using an FAC system in which the net FAC cells (upward to the west, downward to the east) are 20°–50° apart in longitude (this study; Samson and Harrold, 1983; Lester et al., 1983). The westward velocity of the Pi 2's FAC is much larger than typical westward velocities of the WTS (typical maxima are ~2–3 km/s, see e.g. Tighe and Rostoker, 1981). Consequently the westward motion of the Pi 2 currents is most likely caused by a mechanism substantially different from that causing the formation of the WTS.

Summary and conclusions

The data from this campaign indicate that Pi 2's are associated with the brightening of an auroral arc at the onset of the substorm expansive phase. In at least some cases, which this study included, the brightening and onset of the expansive phase occur in the region of the eastward electrojet, equatorward of the existing Harang discontinuity.

A comparison of the polarization data from the Pi 2's in this study suggests that the Pi 2's might be associated with a westward-moving, transient reflection of an incident pulse of equatorward electric fields (at ionospheric levels). Although only one pulse was used to model the Pi 2's in this study, subsequent reflections from the magnetospheric source regions (Nishida, 1979; Kan et al., 1982), or the southern polar ionosphere, could lead to a series of westward-moving pulses, giving the longer Pi 2 trains often seen on the ground. However, the westward motion must be an integral part of the model as westward "apparent" phase velocities are seen at mid-latitude stations. In any case, the single transient model presented here should give the simplest possible Pi 2 pulses, with only ~1 cycle observed at mid latitudes in the *H* component as the FAC "wedge" moves westward.

If my conjecture that the source of the electric field transient is in the CPS near the LLBL (see the Discussion), then the Pi 2's might indicate that the distur-

bance leading to the substorm expansive phase is propagating sunward from the outer magnetotail.

If the Pi 2 is typically associated with the brightening of an arc, the westward motion of the Pi 2 might also be accompanied by a rapid westward expansion of the brightening. Because of the high velocities of the expansion (20–50 km/s), typical all-sky camera exposure times (5–20 s) are much too long and it may be necessary to use a television system with an image intensifier in order to observe the dynamic features of this brightening. Westward-propagating brightening with velocities in excess of 10 km/s have already been reported (Opgenoorth et al., 1983) giving some support to the predictions of the Pi 2 model which I have proposed here. A careful correlation of high time resolution (5 s or better) auroral photographs with Pi 2 magnetic signature would help considerably in an evaluation of the transient model.

Acknowledgements. I wish to thank Prof. G. Rostoker for many interesting discussions and talks on the topic of Pi 2's, and Mr. M.G. Connors for his collaboration in the computation of the numerical results for the Pi 2 model. The original programs for computation of the magnetic fields were written by Dr. J.L. Kisabeth. I am grateful to Transport Canada (Telecommunications Branch), Dept. of Environment and Fisheries (Atmospheric Environmental Service - Western Regional Headquarters) and to Mr. and Mrs. Ted Malewski of Fort Providence, N.W.T., for their help in operating the magnetometer array.

The research described in this report was supported in part by the Boreal Institute for Northern Studies of the University of Alberta, the Natural Sciences and Engineering Research Council of Canada and by the U.S. Air Force Geophysics Laboratory (Contract No. F19628-82-k-0032). The author is an NSERC University Research Fellow.

References

Afanasyeva, L.T., Raspopov, O.M., Schepetrov, R.V., Koshelevskiy, V.I., Hazarov, M.D.: Relationship between geomagnetic pulsations of the Pi 2 type and the parameters of the auroral zone. Geomagn. Aeron. **10**, 600–601, 1970

Baumjohann, W., Pellinen, R.J., Opgenoorth, H.J., Nielsen, E.: Joint two-dimensional observations of ground magnetic and ionospheric electric fields associated with auroral zone currents: current systems associated with local auroral breakups. Planet. Space Sci. **29**, 431–447, 1981

Björnsson, A., Hillebrand, O., Voelker, H.: First observational results of geomagnetic Pi 2 and Pc 5 pulsations on a north-south profile through Europe. Z. Geophys. **37**, 1031–1042, 1971

Boström, R.: Mechanisms for driving Birkeland currents. In: Physics of the hot plasma in the magnetosphere, B. Hultqvist and L. Stenflo, eds., 341–362. New York Plenum Press 1975

Brekke, A., Doupnik, J.R., Banks, P.M.: Incoherent scatter measurements of the E region conductivities and currents in the auroral zone. J. Geophys. Res. **79**, 3773–3790, 1974

Eastman, T.E., Hones, E.W. Jr., Bame, S.J., Asbridge, J.R.: The magnetospheric boundary layer: site of plasma, momentum and energy transfer from the magnetosheath into the magnetosphere. Geophys. Res. Lett. **3**, 685–688, 1976

Fejer, J.A., Lee, L.F.: Guided propagation of Alfvén waves in the magnetosphere. J. Plasma Physics **1**, 387–406, 1967

Glaßmeier, K.-H.: On the influence of ionospheres with non-uniform conductivity distribution on hydromagnetic waves. J. Geophys. **54**, 125–137, 1984

Goertz, C.K.: Discrete breakup arcs and kinetic Alfvén waves. In: Physics of auroral arc formation, S.I. Akasofu and J.R. Kan, eds.: pp. 451–455. American Geophysical Union 1981

Goertz, C.K., Boswell, R.W.: Magnetosphere-ionosphere coupling. J. Geophys. Res. **84**, 7239–7246, 1979

Hakura, Y.: Tables and maps of geomagnetic coordinates corrected by the higher order spherical harmonic terms. Report of Ionospheric and Space Res. in Japan **19**, 121–157, 1965

Iijima, T., Petemra, T.A.: The amplitude distribution of field aligned currents at northern high latitudes observed by Triad. J. Geophys. Res. **81**, 2165–2174, 1976

Kan, J.R.: Energization of auroral electrons by electrostatic shock waves. J. Geophys. Res. **80**, 2089–2095, 1975

Kan, J.R., Longenecker, D.U., Olson, J.V.: A transient response model of Pi 2 pulsation. J. Geophys. Res. **87**, 7483–7488, 1982

Kindel, J.M., Kennel, C.F.: Topside current instabilities. J. Geophys. Res. **76**, 3055–3078, 1971

Kisabeth, J.L.: On calculating magnetic and vector potential fields due to large scale magnetospheric current systems and induced currents in an infinitely conducting earth. In: Quantitative modeling of magnetospheric processes, W.P. Olson, ed.: pp. 473–498, Geophys. Monogr. Ser., **21**. Washington, D.C., 1979

Lester, M., Hughes, W.J., Singer, H.J.: Polarization patterns of Pi 2 magnetic pulsations and the substorm current wedge. J. Geophys. Res. **88**, 7958–7966, 1983

Mallinckrodt, A.J., Carlson, C.W.: Relations between transverse electric fields and field-aligned currents. J. Geophys. Res. **83**, 1426–1432, 1978

Maltsev, Yu.P., Leontyev, S.V., Lyatskiy, V.B.: Generation and natural frequencies of Pi 2 pulsations. Geomagn. Aeron. **14**, 101–107, 1974

McPherron, R.L., Russell, C.T., Aubry, M.P.: Satellite studies of magnetospheric substorms on August 15, 1968. 9, Phenomenological model for substorms. J. Geophys. Res. **78**, 3131–3149, 1973

Mozer, F.S., Cattell, C.A., Hudson, M.K., Lysak, R.L., Temerin, M., Torbert, R.B.: Satellite measurements and theories of low altitude auroral particle acceleration. Space Sci. Rev. **27**, 155–213, 1980

Nishida, A.: Possible origin of transient dusk-to-dawn electric field in the nightside magnetosphere. J. Geophys. Res. **84**, 3409–3412, 1979

Nishida, A.: Geomagnetic diagnosis of the magnetosphere. New York: Springer-Verlag, 1978

Opgenoorth, H.J., Pellinen, R.J., Baumjohann, W., Nielsen, E., Marklund, G., Eliasson, L.: Three dimensional current flow and particle precipitation in a westward travelling surge (observed during the barium-GEOS rocket experiment). J. Geophys. Res. **88**, 3138–3152, 1983

Pashin, A.B., Glaßmeier, K.H., Baumjohann, W., Raspopov, O.M., Yahnin, A.G., Opgenoorth, H.J., Pellinen, R.J.: Pi 2 magnetic pulsations, auroral break-ups, and the substorm current wedge: a case study. J. Geophys. **51**, 223–233, 1982

Pytte, T., Trefall, H.: Auroral-zone electron precipitation event observed before and at the onset of negative magnetic bays. J. Atoms. Terr. Phys. **34**, 315–337, 1972

Pytte, T., McPherron, R.L., Kokubun, S.: The ground signatures of the expansion phase during multiple onset substorms. Planet. Space Sci. **24**, 1115–1132, 1976

Rostoker, G.: Dependence of the high-latitude ionospheric fields and plasma characteristics on the properties of the interplanetary medium. In: High-latitude space plasma physics, B. Hultqvist and T. Hagfors, eds.: p. 189, Plenum Publ. Co., New York, 1983

Rostoker, G.: Implications of the hydrodynamic analogue for the solar terrestrial interaction and the mapping of high latitude correction pattern into the magnetotail. Geophys. Res. Lett. **11**, 251–254, 1984

Rostoker, G., Samson, J.C.: Polarization characteristics of Pi 2 pulsations and implications for their source mechanisms; location of source regions with respect to the auroral electrojets. Planet. Space Sci. **29**, 225–247, 1981

Rostoker, G., Samson, J.C.: Can substorm expansive phase effects and low frequency Pc magnetic pulsations be attributed to the same source mechanism? Geophys. Res. Lett. **11**, 271–274, 1984

Rostoker, G., Armstrong, J.C., Zmuda, A.J.: Field-aligned current flow associated with intrusion of the substorm-intensified westward electrojet into the evening sector. J. Geophys. Res. **25**, 3571–3579, 1975

Rostoker, G., Spadinger, I., Samson, J.C.: Local time variation in the response of Pc 5 pulsations in the morning sector to substorm expansive phase onsets near midnight. J. Geophys. Res. 1984 (in press)

Samson, J.C.: Pi 2 pulsations: high latitude results. Planet. Space Sci. **30**, 1239–1247, 1982

Samson, J.C.: Pure states, polarized waves, and principal components in the spectra of multiple, geophysical time-series. Geophys. J.R. Astron. Soc. **72**, 647–664, 1983a

Samson, J.C.: The reduction of sample bias in polarization estimators for multichannel geophysical data with anisotropic noise. Geophys. J.R. Astron. Soc. **75**, 289–308, 1983b

Samson, J.C., Harrold, B.G.: Maps of the polarizations of high latitude Pi 2's. J. Geophys. Res. **88**, 5736–5744, 1983

Samson, J.C., Rostoker, G.: Polarization characteristics of Pi 2 pulsations and implications for their source mechanism; influence of the westward travelling surge. Planet. Space Sci. **31**, 435–458, 1983

Shawhan, S.D., Fälthammer, C.G., Block, L.P.: On the nature of large auroral zone electric fields at $1-R_E$ altitude. J. Geophys. Res. **83**, 1049–1054, 1978

Sonnerup, B.U.Ö.: Theory of the low latitude boundary layer. J. Geophys. Res. **85**, 2017–2026, 1980

Southwood, D.J., Stuart, W.F.: Pulsations at the substorm onset. In: Dynamics of the magnetosphere, S.-I. Akasofu, ed.: pp. 341–355, D. Reidel, Hingham, MA, 1979

Stix, T.H.: The theory of plasma waves. New York, McGraw-Hill, 1962

Tighe, W.G., Rostoker, G.: Characteristics of westward travelling surges during magnetospheric substorms. J. Geophys. **50**, 51–67, 1981

Troitskaya, J.A., Gul'elmi, A.V.: Geomagnetic micropulsations and diagnostics in the magnetosphere. Space Sci. Rev. **7**, 689–768, 1967

Vondrak, R.R.: Model of Birkeland currents associated with an auroral arc. J. Geophys. Res. **80**, 4011–4014, 1975

Received December 20, 1983; Revised October 12, 1984
Accepted October 25, 1984